

Two-Pulse Ionization Injection into Quasi-Linear Laser Wakefields

Contact: nicolas.bourgeois@physics.ox.ac.uk

N. Bourgeois, J. Cowley, and S. M. Hooker

*Department of Physics,
University of Oxford,
Clarendon Laboratory, Parks Road,
OX1 3PU, United Kingdom*

Abstract

We describe a scheme for controlling electron injection into the quasi-linear wakefield driven by a guided drive pulse via ionization of a dopant species by a collinear injection laser pulse with a short Rayleigh range. The scheme is analyzed by particle in cell simulations which show controlled injection and acceleration of electrons to an energy of 370 MeV, a relative energy spread of 2%, and a normalized transverse emittance of $2.0 \mu\text{m}$.

This is a CLF report version of the original APS paper. It should be cited as N. Bourgeois, J. Cowley, and S. M. Hooker, *Phys. Rev. Lett.* 111, 155004 (2013). APS link here: <http://link.aps.org/doi/10.1103/PhysRevLett.111.155004>

1 Introduction

Laser-driven plasma accelerators can accelerate charged particles to relativistic energies with acceleration gradients at least three orders of magnitude greater than possible in a conventional, radio-frequency device [1]. Impressive progress has been made in recent years, with several groups reporting the generation of beams of electrons with energies in the GeV range [2, 3, 4, 5, 6, 7, 8, 9].

In most experiments to date the accelerated electrons originate in the target plasma and are trapped in a highly nonlinear plasma wakefield by wave-breaking. With careful control of the driving laser and target plasma it is possible to generate beams with relative energy spread and shot-to-shot reproducibility at the level of several percent [10, 11, 12, 13], but it is recognized that better control of the injection process would significantly improve the values of, and reduce the fluctuations in, the electron bunch parameters.

Several techniques for controlling electron injection have been described, including colliding-pulse injection, [14] density ramp injection [15, 16, 17], ionization injection [18, 19] and injection controlled with an external magnetic field [20]. However, to date these techniques have only been demonstrated to control injection into nonlinear wake fields.

It would be advantageous also to be able to control the injection of particles into linear or quasi-linear wakefields, which arise for driving laser pulses with a peak normalized vector potential $a_0 \lesssim 1$. The linear regime

offers several advantages: the range of phases available for acceleration is equal for positive and negative particles, allowing, for example, acceleration of electrons and positrons; self-injection is avoided, preventing unwanted dark current; relativistic self-focusing of the driving laser pulse can be avoided, allowing intensity-independent guiding of the driving laser pulse in a plasma channel and control of the particle energy gain through adjustment of the laser intensity.

In this letter we consider an extension of the ionization injection scheme with a single pulse to the case of linear or quasi-linear wakefields. With single-pulse ionization injection, partially-ionized species within the plasma are ionised by the driving laser pulse, and these additional electrons can become trapped in the plasma wakefield. Chen et al. [21] have recently shown that trapping does not occur for resonant Gaussian laser pulses with a peak normalized vector potential $a_0 \lesssim 1.7$; in its simplest form, therefore, ionization injection will not occur in linear wakefields. The reason for this is that ionization will principally occur on the leading edge of the driving laser pulse, but for the ionised electrons to be trapped they must be born in a phase of the plasma wave for which the plasma potential Φ is sufficiently positive. For intense laser pulses, and hence nonlinear wakefields, the regions of ionization and the trapping partially overlap, but for linear wakefields this is not the case.

The method described here is also related to the LILAC scheme described by Umstadter et al. [22, 23] in which an injection laser pulse is used to promote injection of electrons into the wakefield produced by a driving laser pulse. Both transverse and collinear geometries have been considered. The LILAC scheme differs from the 2PII scheme in that for LILAC: (i) the mechanisms responsible for injection are considered to be modification of the motion of electrons within the wakefield, and of the wakefield itself [24], by the ponderomotive force of the injection laser; (ii) the intensity of the driving pulse is relatively high ($a_0 \geq 1.5$) and hence produces a nonlinear wakefield. We note that in their work Umstadter et al. mention that photoionization could be used to control injection, but they do not analyze this case.

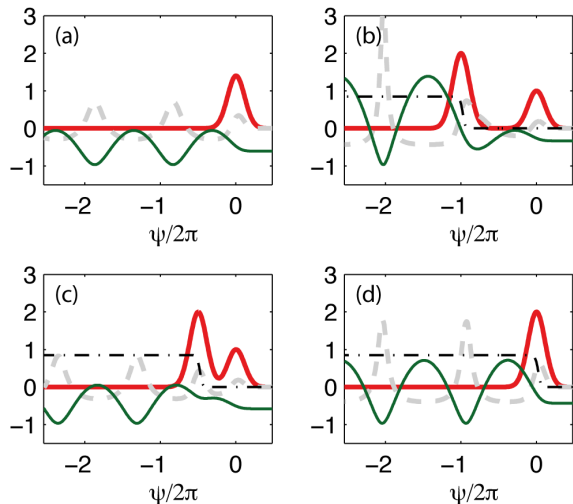


Figure 1: One-dimensional fluid simulations of the electron density (gray, dashed), trapping parameter $\Delta\mathcal{H}$ (green, thin solid), and fractional ionization of N^{5+} ions (black, dash-dot) produced by: (a) a single laser pulse with a peak normalized vector potential $a_{\text{drive}} = 1.3$; and a pair of laser pulses with $a_0^{\text{drive}} = 1.0$ and $a_0^{\text{inj}} = 2$ and a relative delay of $\Delta t = 2\pi/\omega_p$ (b), $\Delta t = \pi/\omega_p$ (c), and $\Delta t = 0$ (d). For all plots the laser pulses (red, thick solid) have a Gaussian temporal profile of rms duration $\tau_{\text{rms}} = 1/k_p c$.

2 Simulations

In order to understand the operation of the 2PII scheme in more detail we first consider the one-dimensional (1D) motion of electrons within a wakefield. This motion is determined by the Hamiltonian $\mathcal{H}(u, \psi) = (\gamma_{\perp}^2 + u^2)^{1/2} - \beta_p u - \phi(\psi)$, where $\gamma = (\gamma_{\perp}^2 + u^2)^{1/2}$ is the Lorentz factor of the electron, $u = \gamma\beta$ is the normalized longitudinal momentum, β_p is the normalized phase velocity of the plasma wave, and $\psi = k_p(x - \beta_p t)$. Here $k_p = \omega_p/c$, $\phi(\psi) = e\Phi/m_e c^2$, and the angular plasma frequency is $\omega_p = (n_e e^2/m_e \epsilon_0)^{1/2}$. An electron born at rest has $\mathcal{H} = \mathcal{H}_i = 1 - \phi(\psi_i)$; trapping requires [21] $\Delta\mathcal{H} = \mathcal{H}_s - \mathcal{H}_i > 0$ where the separatrix $\mathcal{H}_s = \gamma_{\perp}(\psi_{\text{min}})/\gamma_p - \phi(\psi_{\text{min}})$ in which $\phi(\psi_{\text{min}})$ is the potential of the plasma wave at the trapping phase ψ_{min} .

Figure 1 shows wakefields calculated from the 1D fluid equations, within the quasi-static approximation, for the case of laser pulses with a Gaussian temporal profile of root-mean-square (rms) duration $\tau_{\text{rms}} = 1/k_p c$. Also shown is the fractional ionisation of nitrogen atoms, calculated from the ADK ionization rates [25]. We choose nitrogen as a dopant since for the laser parameters considered low ionization stages will be ionized by the leading edge of the driving pulse, but N^{n+} ions with $n \geq 5$ can only be ionized near the peak of the injection pulse. Figure 1(a) shows the wakefield driven by a *single* laser

pulse with a peak normalized vector potential $a_0 = 1.3$. In agreement with earlier work by Chen et al. [21], it is clear that ionized electrons cannot be trapped since $\Delta\mathcal{H} < 0$ for all phases ψ .

Figure 1(b) - (d) shows how a second, collinear laser pulse may be used to trap electrons within the wakefield of a lower intensity drive pulse. In these simulations the amplitude of the injection pulse is $a_0^{\text{inj}} = 2$, which is sufficiently high to ionize N^{5+} ions. In Figure 1(b), the delay between the two pulses corresponds to a phase delay $\Delta\psi_{\text{inj}} = 2\pi$, and hence the wakefields driven by the two laser pulses reinforce each other. Now electrons are ionized from the dopant in regions for which $\Delta\mathcal{H} > 0$, and hence they will be trapped. Figure 1(c) shows that electrons will also be ionized and trapped for $\Delta\psi_{\text{inj}} = \pi$; however, in this case the trapping is weak since the wakefields driven by the two pulses partially cancel each other. Figure 1(d) shows the case for $\Delta\psi_{\text{inj}} = 0$ and drive and injection pulses with $a_0^{\text{inj}} = a_0^{\text{drive}} = 1$, which is equivalent to a single pulse with $a_0^{\text{drive}} = 2$. In agreement with [21], this shows that the injection pulse of Figs 1(b) and (c) would be sufficient for ionization trapping on its own — albeit without the advantages of greater control and localized injection of the 2PII scheme — since there exists a small window within which ionization occurs and $\Delta\mathcal{H} > 0$.

To obtain a more detailed quantitative understanding we have performed 2D particle-in-cell simulations using the OSIRIS code [26]. In these simulations the drive and injection laser pulses had a Gaussian temporal profile with $k_p c \tau_{\text{rms}} = 1$, and Gaussian transverse profiles of spot size ($1/e^2$ radius) $w_0^{\text{drive}} = 30 \mu\text{m}$ and $w_0^{\text{inj}} = 8 \mu\text{m}$ respectively. The two pulses were focused at the entrance of a plasma channel with an axial electron plasma density of $n_e(0) = 2.0 \times 10^{18} \text{cm}^{-3}$, with a parabolic transverse density profile matched to the spot size of the driving pulse. The boundary between the entrance to the plasma channel and vacuum took the form of a linear ramp of length $15c/\omega_p \approx 60 \mu\text{m}$ which was sufficiently long to avoid unwanted self injection at the vacuum-plasma boundary. Neutral nitrogen atoms, with a density equal to 5% of the initial axial electron density were distributed uniformly throughout the plasma; the nitrogen concentration was chosen to be sufficient to provide a reasonable number of trapped electrons without leading to distortion of the plasma channel following ionization of low-charge states by the driving laser pulse. A moving window of $95 \times 450 \mu\text{m}$ was used with a 2500×750 grid, with 4 particles per cell for the plasma and 2500 particles per cell for the nitrogen atoms. The charge of the electrons ionized from the nitrogen atoms was deposited using a quadratic interpolation scheme.

Figures 2(a), 2(b) and 2(c) show, at various points z along the plasma, the densities of electrons in the hydrogen plasma channel and from ionization of N^{n+} ions with $n \geq 5$. Figure 2(a) shows electrons being ionized

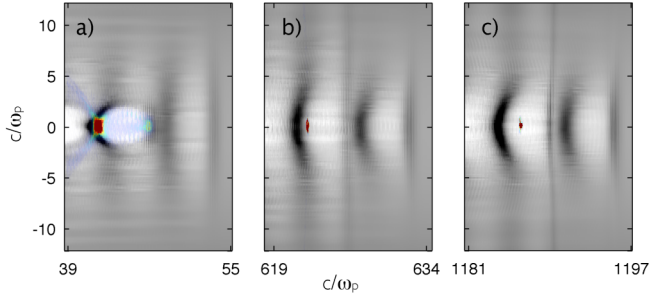


Figure 2: Calculated density of electrons for (a) $z = 0.2$ mm and 2.3 mm and (c) 4.5 mm. Shown in grayscale are electrons ionized from hydrogen and $N^{<5+}$ ions; the color scale shows electrons ionized from $N^{\geq 5+}$ ions. Laser-plasma parameters are $n_e(0) = 2 \times 10^{18} \text{ cm}^{-3}$, injection pulse $a_0 = 2$ and drive pulse $a_0 = 1$; both laser pulses have a Gaussian temporal profile with $L = k_p c \tau_{\text{rms}}$.

from the N^{n+} ions near the axis and slipping backwards relative to the wakefield. Some of these electrons are trapped at the rear of the second plasma period behind the driving pulse — but others continue to slip back to form a cone of ejected electrons. In Fig. 2(b), the intensity of the injection pulse has been reduced by diffraction sufficiently for ionization of $N^{\geq 5+}$ ions to cease; a well defined electron bunch has started to form at the rear of the plasma period, with a few electrons still slipping out of this bucket in a cone of larger angle, reflecting their larger forward momentum. The electron bunch is then accelerated in the wakefield, with little further loss of electrons, as shown in Fig. 2(c). The total charge in the bunch is 5 pC . A detailed analysis of the simulations shows that the only electrons which are trapped and accelerated are those ionized by the injection pulse from N^{n+} ions with $n \geq 5$.

Figure 3 shows, for the same laser-plasma parameters as in Fig. 2, the phase space distribution and energy spectrum of electrons ionized from N^{n+} ions, with $n \geq 5$. As expected, the injected electrons are first trapped at the back of the second plasma period behind the driving pulse; they move forward relative to the wakefield as they gain energy; and phase-rotation near the point of dephasing reduces the energy spread of the trapped bunch. The maximum electron bunch energy is approximately 370 MeV . In these simulations a second group of low energy, low charge electrons is injected close to the point of dephasing of the main bunch due to ionization by the the diffracted, but temporally compressed injection pulse; other simulations show that reducing the plasma density slightly prevents this second injection event.

Figure 4 shows the evolution along the plasma accelerator of the emittance and energy spread of electrons ionized from $N^{\geq 5+}$ for drive ($a_0 = 1$) and injection ($a_0 = 2$)

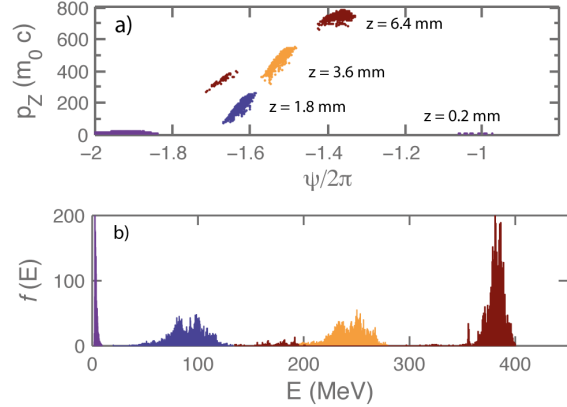


Figure 3: Calculated phase space distribution (a) and energy spectrum (b) of electrons ionized from N^{n+} ions, with $n \geq 5$, at distances of $z = 0.2$ mm, 1.8 mm, 3.6 mm and 6.4 mm of acceleration. Only electrons remaining in the simulation box are included.

laser pulses of identical duration equal to (a, c) $k_p c \tau_{\text{rms}} = 1$ and (b, d) $k_p c \tau_{\text{rms}} = 2.2$. The normalized rms transverse emittance of the accelerated electron bunch is calculated [27] from $\epsilon_{n,\text{rms}} = \sqrt{\langle x^2 \rangle \langle p_x^2 \rangle - \langle x p_x \rangle^2}$ where x is the transverse position and p_x is the transverse momentum normalised to $m_e c$. Here the symbol $\langle \rangle$ denotes the second central moment, i.e. $\langle xy \rangle = \overline{xy} - \overline{x} \overline{y}$ in which the bar indicates the average over particles. The geometric emittance [27] is calculated from $\epsilon_{\text{rms}} = \epsilon_{n,\text{rms}} / \overline{p}_z$ where \overline{p}_z is the average longitudinal momentum normalised to $m_e c$.

Figure 4(a) shows that ϵ_{rms} increases rapidly until $z = 200 \mu\text{m}$ whilst new nitrogen electrons are ionized and some of these slip backwards in the wakefield. After the intensity of the injection pulse has reduced sufficiently for ionization of $N^{\geq 5+}$ to stop, ϵ_{rms} decreases approximately as $1/\gamma$ — where γ is the mean relativistic factor of the trapped electrons — which is consistent with the normalised emittance of the bunch not varying significantly as it is accelerated. The final normalized emittance reaches $2.0 \mu\text{m}$ at $z \approx 6.0 \text{ mm}$, close to the point of maximum electron energy. The rms energy spread ΔE_{rms} of electrons ionized from $N^{\geq 5+}$ initially increases rapidly as the number of these electrons increases, before increasing more slowly and then decreasing as the electron bunch rotates in phase space. The relative energy spread decreases even before ionization ceases, since it is dominated by the increase in γ ; a minimum value of $\Delta E_{\text{rms}}/E = 2\%$ is reached just after the point of dephasing.

The effect of using longer drive and injection pulses is shown in Figure 4(b, d). The main difference is that the interaction of the bunch with the tail of the injection pulse causes the transverse emittance to increase before the dephasing point is reached. As a result a minimum value of $\epsilon_{n,\text{rms}} = 2.0 \mu\text{m}$ is reached at $z = 1.0 \text{ mm}$; this

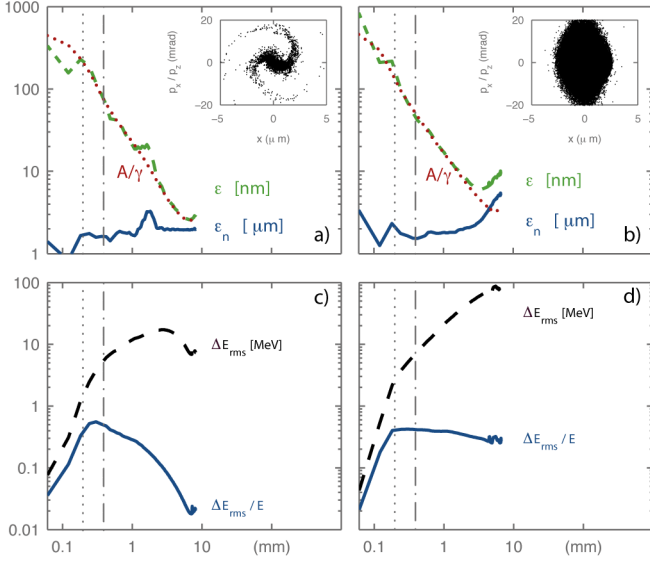


Figure 4: Evolution with position z of the drive laser pulse along the plasma channel of the parameters of electrons ionized from $N^{\geq 5+}$ for drive and injection laser pulses with identical duration equal to (a, c) $k_p c \tau_{rms} = 1$ and (b, d) $k_p c \tau_{rms} = 2.2$. Shown are the relative energy spread $\Delta E_{rms}/E$ (blue, solid) and ΔE_{rms} (black, dashed), where ΔE_{rms} is the rms energy spread, the geometric emittance ϵ_{rms} (green, dashed), and normalised emittance $\epsilon_{n,rms}$ (blue, solid). Also shown is a plot of A/γ (red, dotted), where γ is the mean relativistic factor of the trapped electrons, with the parameter A adjusted to fit the minimum value of ϵ_{rms} . The inset shows the beam transverse distribution of the electron bunch at the point where the energy spread is minimum. The dotted vertical line shows where injection stops and the dotted dashed vertical line shows where the mean velocity of the injected electrons first exceeds the phase velocity of the plasma wakefield. Only electrons in the first injected bunch which remain in the simulation box are included in calculations of these parameters.

increases to $\epsilon_{n,rms} = 5 \mu\text{m}$ at the point of minimum relative energy spread.

3 Conclusion

In summary, we have proposed a new scheme for controlling the injection and trapping of electrons into a quasi-linear laser-driven wakefield. Non-optimized numerical simulations show that this method can generate electron bunches of charge 5 pC, mean energy 370 MeV, relative energy spread of 2%, and a normalized emittance of 2.0 μm .

We note that the energy spread might be reduced still further by employing simultaneous space-time focussing (SSTF) [28, 29] for the injection pulse, which could substantially reduce the distance over which the intensity

of the pulse remains high. In practice reduction of the depth of focus by an order of magnitude is possible, and additional control can be achieved by combining SSTF with Bessel beam generation [30]. These methods would further constrain the region in which injection occurs, without reducing the spot size of the injection pulse to unpractically small values or to values for which the trapped charge is small.

Acknowledgments

This work was supported by the Engineering and Physical Sciences Research Council (grant no. EP/H011145/1) and by The Leverhulme Trust (grant no. F/08 776/G). The authors would like to acknowledge the OSIRIS Consortium, consisting of UCLA, IST (Lisbon, Portugal), and USC, for the use of OSIRIS, and IST for providing access to the OSIRIS 2.0 framework. We also acknowledge helpful discussions with R.M.G.M. Trines and are grateful for computing resources provided by STFC's e-Science facility.

References

- [1] T. Tajima and J. M. Dawson, "Laser electron-accelerator," *Phys. Rev. Lett.*, vol. 43, no. 4, pp. 267–270, 1979.
- [2] W. P. Leemans, B. Nagler, A. J. Gonsalves, C. S. Tóth, K. Nakamura, C. G. R. Geddes, E. Esarey, C. B. Schroeder, and S. M. Hooker, "GeV electron beams from a centimetre-scale accelerator," *Nat. Phys.*, vol. 2, no. 10, pp. 696–699, 2006.
- [3] S. Karsch, J. Osterhoff, A. Popp, T. P. Rowlands-Rees, Z. Major, M. Fuchs, B. Marx, R. Horlein, K. Schmid, L. Veisz, S. Becker, U. Schramm, B. Hidding, G. Pretzler, D. Habs, F. Gruner, F. Krausz, and S. M. Hooker, "GeV-scale electron acceleration in a gas-filled capillary discharge waveguide," *New J. Phys.*, vol. 9, p. 415, Nov 21 2007.
- [4] T. P. A. Ibbotson, N. Bourgeois, T. P. Rowlands-Rees, L. S. Caballero, S. I. Bajlekov, P. A. Walker, S. Kneip, S. P. D. Mangles, S. R. Nagel, C. A. J. Palmer, N. Delerue, G. Doucas, D. Urner, O. Chekhlov, R. J. Clarke, E. Divall, K. Ertel, P. S. Foster, S. J. Hawkes, C. J. Hooker, B. Parry, P. P. Rajeev, M. J. V. Streeter, and S. M. Hooker, "Laser-wakefield acceleration of electron beams in a low density plasma channel," *Phys. Rev. ST Accel. Beams*, vol. 13, p. 031301, Mar 2010.
- [5] S. Kneip, S. Nagel, S. Martins, S. Mangles, C. Bellei, O. Chekhlov, R. Clarke, N. Delerue, E. Divall, G. Doucas, K. Ertel, F. Fiuza, R. Fonseca, P. Foster, S. Hawkes, C. Hooker, K. Krushelnick, W. Mori, C. Palmer, K. Phuoc, P. Rajeev, J. Schreiber,

- M. Streeter, D. Urner, J. Vieira, L. Silva, and Z. Najmudin, "Near-GeV Acceleration of Electrons by a Nonlinear Plasma Wave Driven by a Self-Guided Laser Pulse," *Physical Review Letters*, vol. 103, p. 035002, July 2009.
- [6] B. Pollock, C. Clayton, J. Ralph, F. Albert, A. Davidson, L. Divol, C. Filip, S. Glenzer, K. Herpoldt, W. Lu, K. Marsh, J. Meinecke, W. Mori, A. Pak, T. Rensink, J. Ross, J. Shaw, G. Tynan, C. Joshi, and D. Froula, "Demonstration of a narrow energy spread, 0.5 GeV electron beam from a two-stage laser wakefield accelerator," *Physical Review Letters*, vol. 107, July 2011.
- [7] J. S. Liu, C. Q. Xia, W. T. Wang, H. Y. Lu, C. Wang, A. H. Deng, W. T. Li, H. Zhang, X. Y. Liang, Y. X. Leng, X. M. Lu, C. Wang, J. Z. Wang, K. Nakajima, R. X. Li, and Z. Z. Xu, "All-Optical Cascaded Laser Wakefield Accelerator Using Ionization-Induced Injection," *Physical Review Letters*, vol. 107, p. 035001, July 2011.
- [8] M. Z. Mo, A. Ali, S. Fourmaux, P. Lassonde, J. C. Kieffer, and R. Fedosejevs, "Quasimonoenergetic electron beams from laser wakefield acceleration in pure nitrogen," *Applied Physics Letters*, vol. 100, no. 7, p. 074101, 2012.
- [9] X. Wang, R. Zgadzaj, N. Fazel, Z. Li, S. A. Yi, X. Zhang, W. Henderson, Y. Y. Chang, R. Korzekwa, H. E. Tsai, C. H. Pai, H. Quevedo, G. Dyer, E. Gaul, M. Martinez, A. C. Bernstein, T. Borger, M. Spinks, M. Donovan, V. Khudik, G. Shvets, T. Ditmire, and M. C. Downer, "Quasimonoenergetic laser-plasma acceleration of electrons to 2GeV," *Nature Communications*, vol. 4, June 2013.
- [10] S. P. D. Mangles, C. D. Murphy, Z. Najmudin, A. G. R. Thomas, J. L. Collier, A. E. Dangor, E. J. Divall, P. S. Foster, J. G. Gallacher, C. J. Hooker, D. A. Jaroszynski, A. J. Langley, W. B. Mori, P. A. Norreys, F. S. Tsung, R. Viskup, B. R. Walton, and K. Krushelnick, "Monoenergetic beams of relativistic electrons from intense laser-plasma interactions," *Nature*, vol. 431, pp. 535–538, Sep 30 2004.
- [11] C. G. R. Geddes, C. Tóth, J. van Tilborg, E. Esarey, C. B. Schroeder, D. Bruhwiler, C. Nieter, J. Cary, and W. P. Leemans, "High-quality electron beams from a laser wakefield accelerator using plasma-channel guiding," *Nature*, vol. 431, pp. 538–541, Sep 30 2004.
- [12] J. Faure, Y. Glinec, A. Pukhov, S. Kiselev, S. Gordienko, E. Lefebvre, J. P. Rousseau, F. Burgy, and V. Malka, "A laser-plasma accelerator producing monoenergetic electron beams," *Nature*, vol. 431, pp. 541–544, Sep 30 2004.
- [13] J. Osterhoff, A. Popp, Z. Major, B. Marx, T. P. Rowlands-Rees, M. Fuchs, M. Geissler, R. Hoerlein, B. Hidding, S. Becker, E. A. Peralta, U. Schramm, F. Gruener, D. Habs, F. Krausz, S. M. Hooker, and S. Karsch, "Generation of stable, low-divergence electron beams by laser-wakefield acceleration in a steady-state-flow gas cell," *Phys. Rev. Lett.*, vol. 101, p. 085002, Aug 22 2008.
- [14] J. Faure, C. Rechatin, A. Norlin, A. Lifschitz, Y. Glinec, and V. Malka, "Controlled injection and acceleration of electrons in plasma wakefields by colliding laser pulses," *Nature*, vol. 444, pp. 737–739, Dec. 2006.
- [15] S. Bulanov, N. Naumova, F. Pegoraro, and J. Sakai, "Particle injection into the wave acceleration phase due to nonlinear wake wave breaking," *Physical Review E*, vol. 58, no. 5, pp. 5257–5260, 1998.
- [16] A. J. Gonsalves, K. Nakamura, C. Lin, D. Panasenkov, S. Shiraishi, T. Sokollik, C. Benedetti, C. Schroeder, C. Geddes, J. van Tilborg, J. Osterhoff, E. Esarey, C. Tóth, and W. P. Leemans, "Tunable laser plasma accelerator based on longitudinal density tailoring," *Nat Phys*, vol. 7, Aug. 2011.
- [17] K. Schmid, A. Buck, C. Sears, J. Mikhailova, R. Tautz, D. Herrmann, M. Geissler, F. Krausz, and L. Veisz, "Density-transition based electron injector for laser driven wakefield accelerators," *Physical Review Special Topics-Accelerators And Beams*, vol. 13, p. 091301, Sept. 2010.
- [18] C. McGuffey, A. G. R. Thomas, W. Schumaker, T. Matsuoka, V. Chvykov, F. J. Dollar, G. Kalintchenko, V. Yanovsky, A. Maksimchuk, K. Krushelnick, V. Y. Bychenkov, I. V. Glazyrin, and A. V. Karpeev, "Ionization Induced Trapping in a Laser Wakefield Accelerator," *Physical Review Letters*, vol. 104, p. 025004, Jan. 2010.
- [19] A. Pak, K. A. Marsh, S. F. Martins, W. Lu, W. B. Mori, and C. Joshi, "Injection and Trapping of Tunnel-Ionized Electrons into Laser-Produced Wakes," *Physical Review Letters*, vol. 104, p. 025003, Jan. 2010.
- [20] J. Vieira, S. F. Martins, V. B. Pathak, R. A. Fonseca, W. B. Mori, and L. O. Silva, "Magnetic Control of Particle Injection in Plasma Based Accelerators," *Physical Review Letters*, vol. 106, p. 225001, May 2011.
- [21] M. Chen, E. Esarey, C. Schroeder, C. Geddes, and W. P. Leemans, "Theory of ionization-induced trapping in laser-plasma accelerators," *Physics of Plasmas*, vol. 19, no. 3, pp. 033101–033101–12, 2012.

- [22] D. Umstadter, J. K. Kim, and E. Dodd, “Laser injection of ultrashort electron pulses into wakefield plasma waves,” *Phys. Rev. Lett.*, vol. 76, pp. 2073–2076, Mar 18 1996.
- [23] E. Dodd, J. K. Kim, and D. Umstadter, “Ultrashort-pulse relativistic electron gun/accelerator,” in *Advanced Accelerator Concepts*, p. 106, The American Institute of Physics, 1997.
- [24] R. G. Hemker, K.-C. Tzeng, W. B. Mori, C. E. Clayton, and T. Katsouleas, “Computer simulations of cathodeless, high-brightness electron-beam production by multiple laser beams in plasmas,” *Physical Review E*, vol. 57, no. 5, p. 5920, 1998.
- [25] M. V. Ammosov, N. B. Delone, and V. P. Krainov, “Tunnel ionization of complex atoms and of atomic ions in an alternating electromagnetic field,” *Soviet Physics - JETP*, vol. 64, no. 6, pp. 1191–1194, 1986.
- [26] R. A. Fonseca, L. O. Silva, F. S. Tsung, V. K. Decyk, W. Lu, C. Ren, W. B. Mori, S. Deng, S. Lee, T. Katsouleas, and J. C. Adam, “OSIRIS: A three-dimensional, fully relativistic particle in cell code for modeling plasma based accelerators,” *Lecture Notes in Computer Science*, vol. 2331, p. 342, 2002.
- [27] K. Floettmann, “Some basic features of the beam emittance,” *Physical Review Special Topics-Accelerators And Beams*, vol. 6, p. 034202, Mar. 2003.
- [28] G. H. Zhu, J. van Howe, M. Durst, W. Zipfel, and C. Xu, “Simultaneous spatial and temporal focusing of femtosecond pulses,” *Optics Express*, vol. 13, no. 6, pp. 2153–2159, 2005.
- [29] C. G. Durfee, M. Greco, E. Block, D. Vitek, and J. A. Squier, “Intuitive analysis of space-time focusing with double-ABCD calculation,” *Optics Express*, vol. 20, no. 13, pp. 14244–14259, 2012.
- [30] M. Clerici, D. Faccio, E. Rubino, A. Lotti, A. Couairon, and P. Di Trapani, “Space-time focusing of Bessel-like pulses,” *Optics Letters*, vol. 35, no. 19, pp. 3267–3269, 2010.